Measurement of the Photodissociation Coefficient of NO_2 in the Atmosphere: II, Stratospheric Measurements

S. MADRONICH*, D. R. HASTIE, H. I. SCHIFF, and B. A. RIDLEY*
Department of Chemistry, York University, Downsview, Ontario, Canada M3J 1P3.

Abstract. The photodissociation coefficient of NO_2, J_{NO_2}, has been measured from a balloon platform in the stratosphere. Results from two balloon flights are reported. High Sun values of J_{NO_2} measured were 10.5 ± 0.3 and $10.3 \pm 0.3 \times 10^{-3}$ s^{-1} at 24 and 32 km respectively. The decrease in J_{NO_2} at sunset was monitored in both flights. The measurements are found to be in good agreement with calculations of J_{NO_2} using a simplified isotropic multiple scattering computer routine.

Key words. J_{NO_2}, NO_2 photolysis, atmospheric photochemistry, J_{NO_2} measurement.

1. Introduction

Models for stratospheric chemistry are very sensitive to the photodissociation coefficient (J_{NO_2}) of the reaction

$$NO_2 + h\nu \longrightarrow NO + O. \qquad \text{(R1)}$$

This reaction, along with

$$NO + O_3 \longrightarrow NO_2 + O_2 \qquad \text{(R2)}$$

determines, to a large extent, the partitioning of NO_x in the daytime stratosphere. The mixing ratio of NO_2 in the stratosphere is important for a number of reasons. The reaction

$$NO_2 + O \longrightarrow NO + O_2 \qquad \text{(R3)}$$

is a major sink for 'odd' oxygen. The other major sinks involve HO_x and Cl_x free radicals which are also affected by NO_2 through the coupling reactions:

$$NO_2 + HO + M \longrightarrow HNO_3 + M, \qquad \text{(R4)}$$

$$NO_2 + ClO + M \longrightarrow ClNO_3 + M. \qquad \text{(R5)}$$

* Present Address: National Center for Atmospheric Research, PO Box 3000, Boulder, CO 80307, U.S.A.

Models generally calculate the rate coefficient J_{NO_2} from the expression:

$$J_{NO_2} = \int_\lambda \sigma(\lambda)\,\phi(\lambda)\,F(\lambda)\,d\lambda \qquad (1)$$

where $\sigma(\lambda)$ and $\phi(\lambda)$ are the NO_2 absorption coefficient as a function of wavelength, the quantum efficiency of reaction (R1) and $F(\lambda)$ is the solar flux at the altitude of interest. Reported determinations of $\sigma(\lambda)$ and $\phi(\lambda)$ (JPL, 1982; Madronich *et al.*, 1984) show some systematic differences in values and in temperature dependences. Differences as much as 20% have been reported for the extraterrestrial solar flux in the relevant spectral region (WMO, 1981). The solar flux at any given altitude must be calculated to include attenuation due to absorption of atmospheric gases above that altitude and must also take into account scattered radiation from the atmosphere and reflections from clouds and the surface. The importance of these effects has been described (e.g. Luther and Gelinas, 1976; Mugnai *et al.*, 1979). Model calculations of J_{NO_2} are therefore complex and involve the uncertainties in parameterizing surface and cloud albedo and scattering due to aerosols. A direct measurement of J_{NO_2} is therefore a preferable input to the models, particularly when they are being tested against simultaneously measured partitioning of NO_x mixing ratios.

In a previous publication (Madronich *et al.*, 1983) we described a method for measuring J_{NO_2} with an apparatus designed primarily for measurements from a balloon in the stratosphere. That paper described the apparatus in detail and presented some tropospheric measurements which were compared with calculations and with other tropospheric measurements. In this paper we give only a brief review of the method and present measurements made during two stratospheric flights. The measurements are compared with calculations using two scattering models. No other direct measurements are available for comparison.

2. Experimental

The experimental method is based on the pressure increase which accompanies the photodissociation of NO_2 in a closed quartz cell. The primary photolysis reaction

$$NO_2 + h\nu \longrightarrow NO + O \qquad (R1)$$

is followed by

$$O + NO_2 \longrightarrow NO + O_2 \qquad (R3)$$

to yield a net reaction

$$2NO_2 + h\nu \longrightarrow 2NO + O_2$$

and an increase in pressure within the cell.

Madronich *et al.* (1983) showed that the measured photodissociation coefficient J_M is obtained, from the NO_2 partial pressure P_{NO_2} and the equilibrium constant for dimerization K, via

$$-2J_M t = \ln \frac{p_{NO_2}(t)}{p_{NO_2}(0)} + \frac{4}{K}\left[p_{NO_2}(t) - p_{NO_2}(0)\right] \quad (1)$$

by plotting the right-hand side of Equation (1) against photolysis time t.

The relationship between this measured photodissociation coefficient, J_M, and the actual ambient value, J_{NO_2}, is described in Section 5.

3. Apparatus

The photolysis cell used during the balloon flights is shown schematically in Figure 1 and is described in Madronich *et al.* (1983).

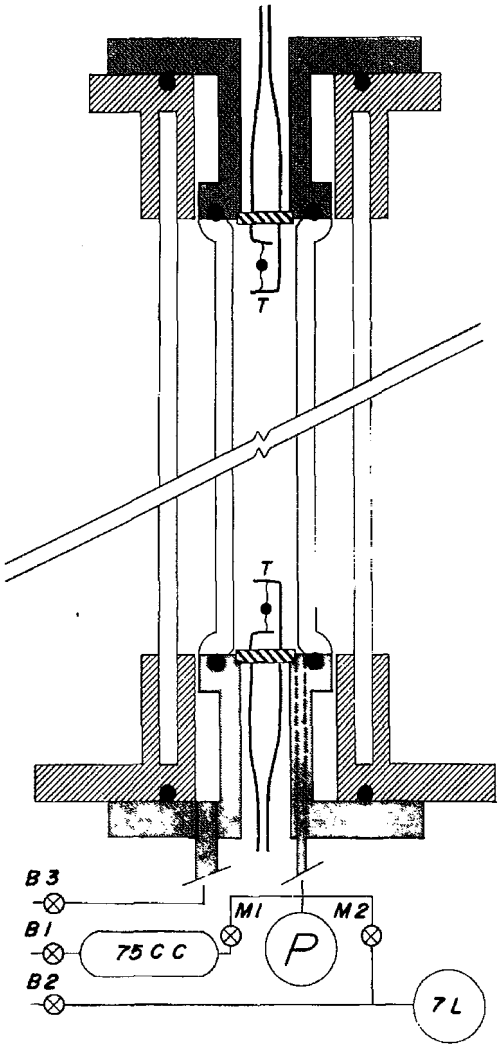

Fig. 1. Schematic of photolysis cell, P – 0 to 5 Torr absolute pressure transducer; T – thermistors; $B1$, $B2$, $B3$ bellows valves (closed during flight); $M1$, $M2$ – latching solenoid valves; 75 cc – volume filled with 70 Torr NO_2; $7L$ – volume evacuated before flight. Not shown is the insulating foam which shadows a small portion of the cell.

To minimize the dimerization of NO_2 to N_2O_4 the cell temperature should be maintained above 260 K. The top and bottom metal flanges are heated and the quartz cell walls heated between experiments by heaters lining the inside of the shutter. The flanges and shutter are insulated to reduce heat loss.

Results from the first flight (Section 5) showed a significant heat loss through the top flange, giving an average cell temperature decrease of 1 C°/min during an experiment. For the second flight additional heating and insulation effectively eliminated the cooling during a photolysis experiment.

The instrument electronics are designed to allow ground activated control of the solenoid valves, the shutter mechanism, and the heaters. The cell pressure, the temperature at several locations in the instrument, the shutter position, and the status of the valves are all telemetered to the ground, where they are recorded on a strip chart recorder.

It is important that the cell receives actinic flux unperturbed by the balloon or its payload. Consequently, the payload is located 55 m below the balloon and the 15 kg instrument lowered a further 5 m below the payload with the photolysis cell in a vertical position. In this configuration, light reflected into the cell by the balloon and the gondola is negligible. Neither the balloon nor the gondola are of sufficient angular extent to interfere with the observation of direct sunlight. Mechanical supports and insulation are painted flat black to prevent any light from entering the cell at angles close to the cell axis. Shadowing of direct and diffuse light by the end flanges and insulation is considered in detail in Section 5.

4. Description of the Balloon Flights

Measurements of J_{NO_2} were made from two balloon flights launched at Gimli, Manitoba (50° 37'N, 97°02'W) in the summer of 1980.

The first balloon, (15,600 m^3), was launched on 22 July 1980, at 02:20 LT (07:20 GMT). The float altitude of 24 km was reached at about 06:00 LT (11:00 GMT) and was maintained to within 1 km until 16:30 LT (21:30 GMT). All of the J_{NO_2} measurements were obtained at this altitude. The balloon travelled well south of Lakes Winnipeg and Manitoba, over largely agricultural terrain. The horizontal trajectory of the balloon is shown in Figure 2a.

The second balloon (101,900 m^3) was launched at 13:54 LT (18:54 GMT) on 2 August 1980, and maintained a float altitude of about 32 km between 16:00 LT (21:00 GMT) and 21:40 LT (02:40 3 August GMT), when the J_{NO_2} experiments were performed. The balloon trajectory, shown in Figure 2b, extended from the southern tip of Lake Winnipeg, along the southern shore of Lake Manitoba, and over agricultural areas of Western Manitoba.

Cloud conditions were estimated from satellite photographs and from surface reports at local airports. On 22 July the sky was mostly clear, with at most two tenths cumulus coverage. However, a large stratocumulus cloud formation was present about 100 km North of the balloon trajectory. On 2 August *ca.* 3/10 cumulus was present during the early part of the flight but dissipated sometime after 18:00 LT (23:00 GMT). A large

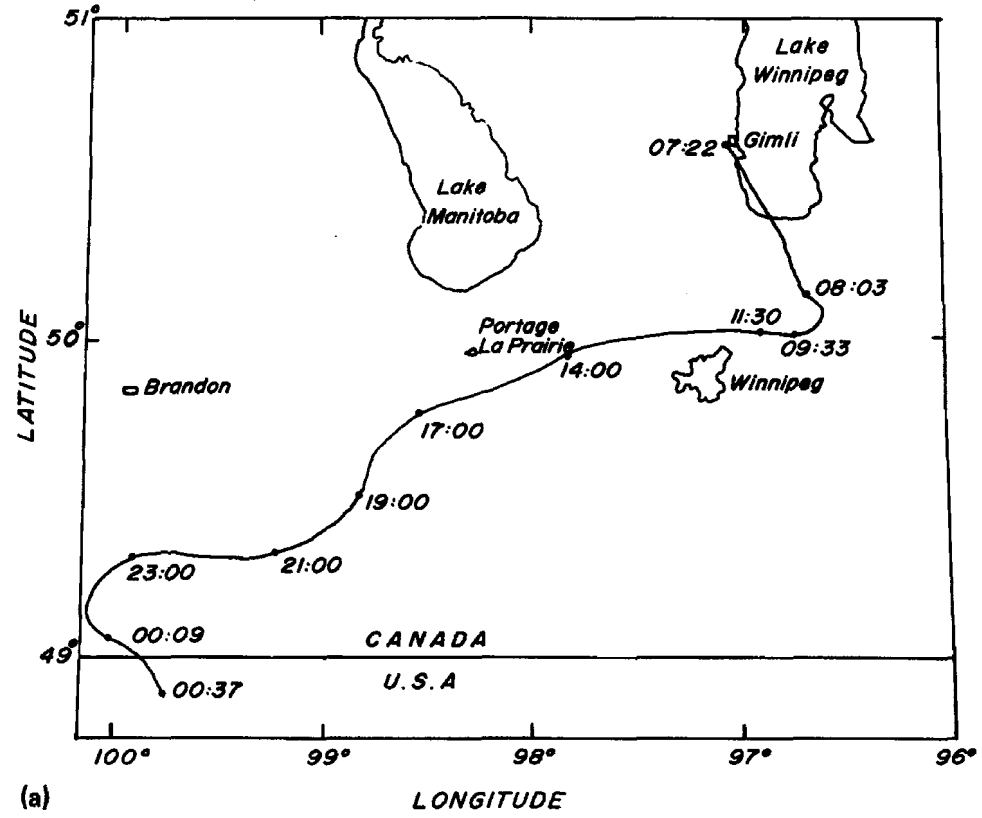

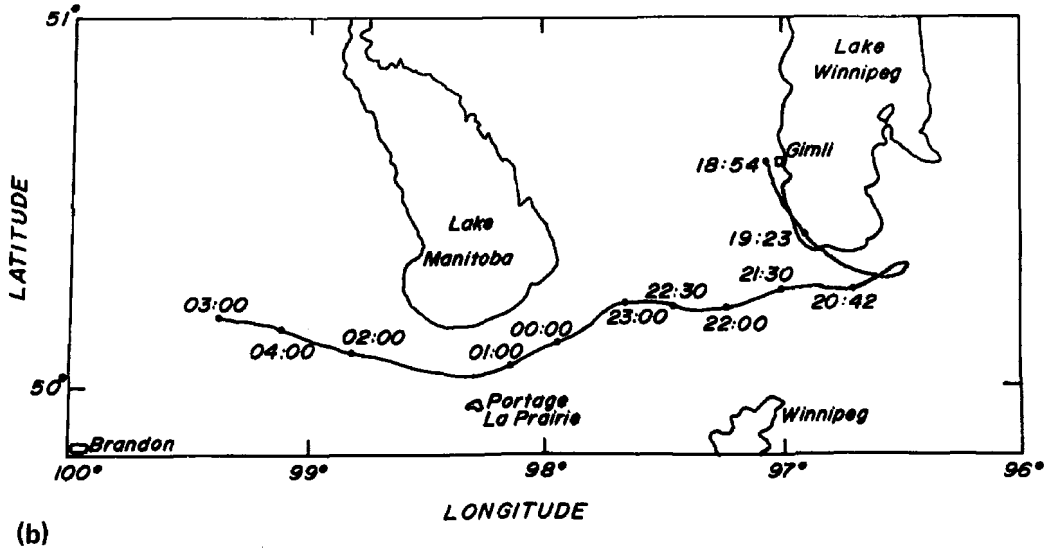

Fig. 2. Balloon trajectories, times indicated are GMT. (a) Flight 1, 22 July 1980; (b) Flight 2, 2 August 1980.

eastward moving cirrus cloud was on the Saskatchewan-Manitoba border during launch, and met the westward moving balloon over Lake Manitoba at *ca.* 19:00 LT (00:00 GMT).

5. Description of the J_{NO_2} Experiments

On 22 July 1980 (Flight 1), the photolysis measurements were delayed to allow the instrument to warm up after the very low temperatures encountered during the night-time ascent through the tropopause. Thus, only high Sun measurements were obtained. Figure 3a shows a typical pressure increase curve as received at the ground station during this flight.

The pressure before the beginning of photolysis showed a slight increase due to N_2O_4 to NO_2 conversion in the warm, low pressure cell. After photolysis the pressure decreased steadily. This decrease also occurred when photolysis experiments were repeated with totally photolysed gases (i.e., NO and O_2). This effect is due to cell cooling, which was

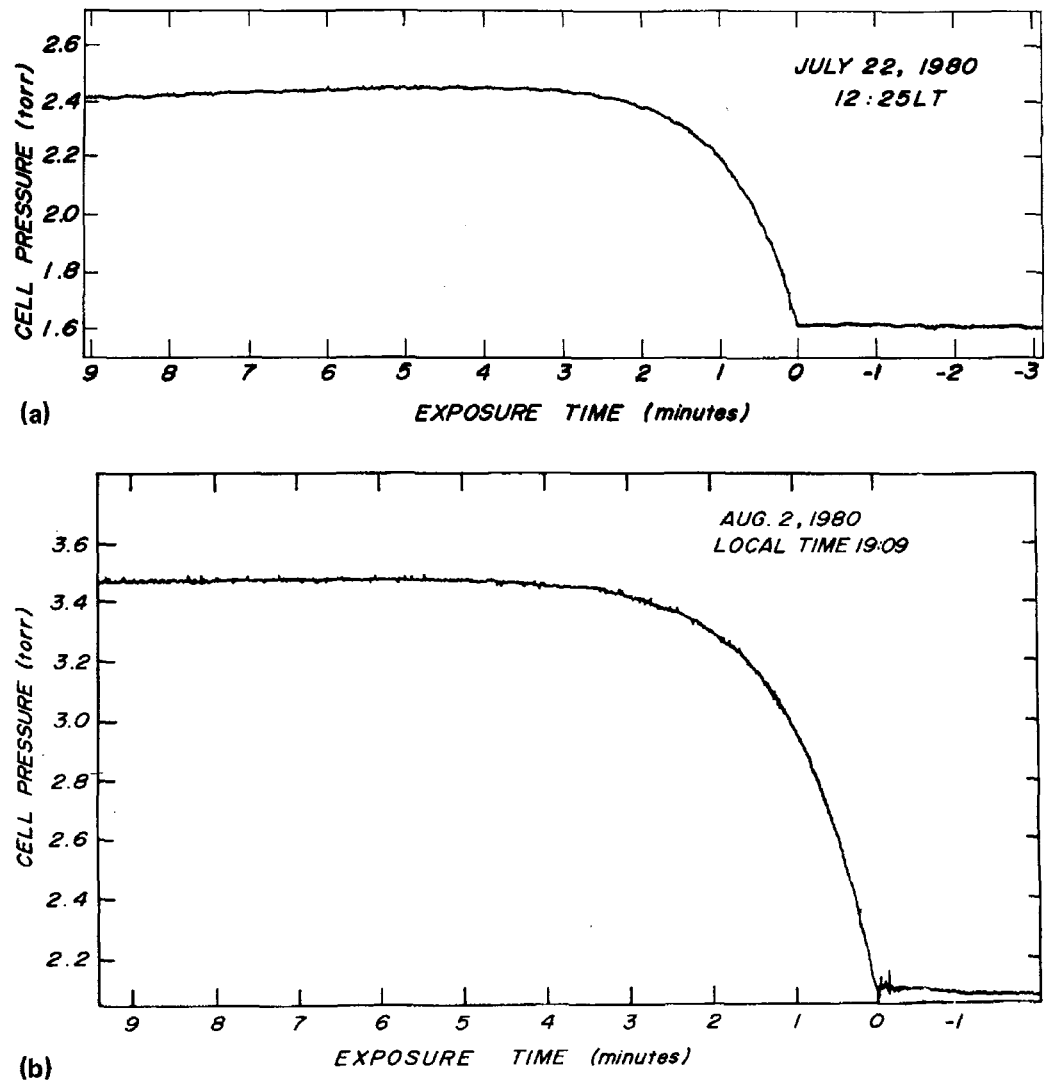

Fig. 3. Typical raw data as received at the ground station. (a) Flight 1, 22 July 1980, 12.25 LT; (b) Flight 2, 2 August 1980, 10.09 LT.

estimated by the pressure drop to be 1°C/min. This value was confirmed by direct temperature measurements with the thermistors.

For flight 2 (2 August 1980) improved heating and a daylight launch allowed measurements immediately after reaching float altitude (32 km), from mid-afternoon through sunset (*ca.* 43° to 90° solar zenith angle). Figure 3b shows a typical pressure increase curve. The pressure decrease after photolysis is absent.

In analyzing the data from flight 1 the pressure was corrected for cell cooling. Otherwise the data analysis is the same as in Madronich *et al.* (1983). Figures 4a and 4b show typical pressure increase data obtained for each flight, analyzed via Equations (1) and (2). It is seen that the predicted linearity is obtained over at least three *e*-folding times. The error bars were obtained from the estimated precision with which the raw pressure data (e.g., Figures 3a and b) could be read from the telemetry chart records, and propagated numerically through Equations (1) and (2). The slope of each plot is $-2J_M$ as attained under the conditions of each experiment.

The photodissociation coefficient J_M obtained from plots such as Figure 4a and 4b pertains to the actinic flux reaching the NO_2 in the quartz photolysis cell, and must now be related to the ambient photodissociation coefficient, J_{NO_2}, by considering the per-

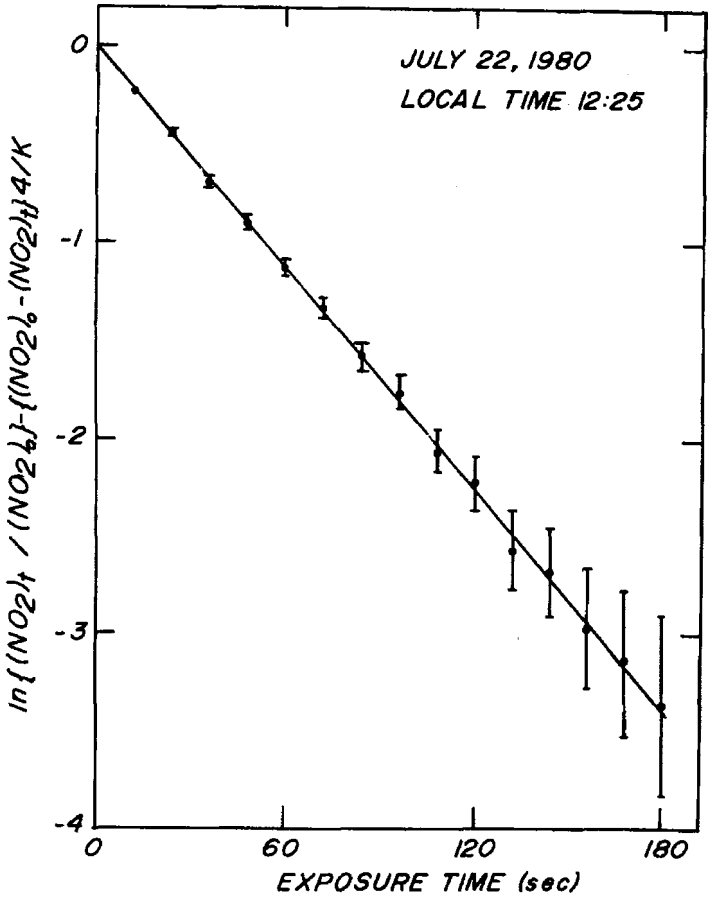

Fig. 4a. Calculations of J_M from the data of Figure 3. Flight 1, 22 July 1980, 12.25 LT.

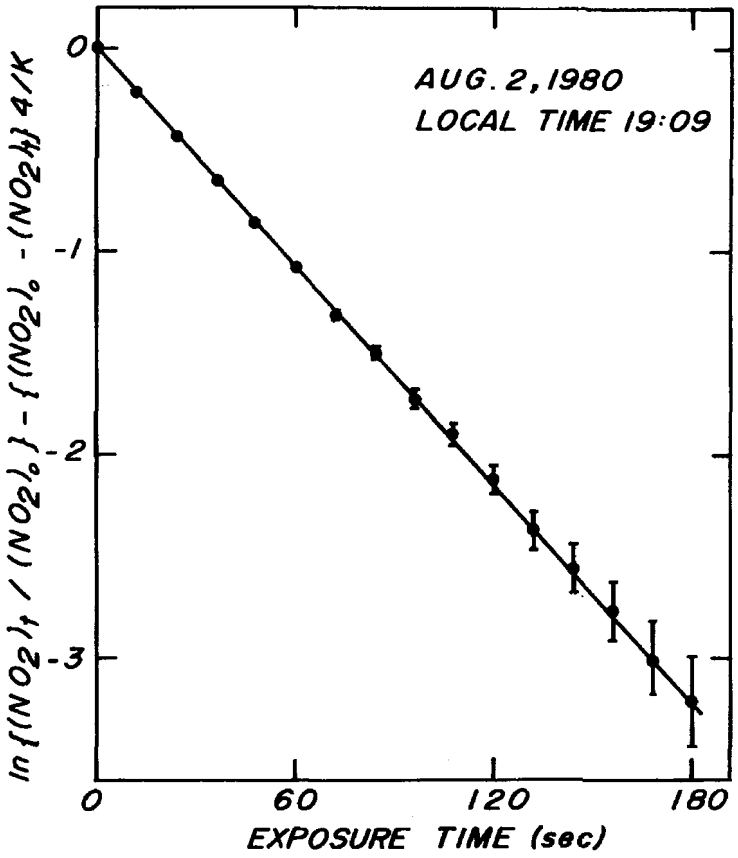

Fig. 4b. Calculation of J_M from the data of Figure 3. Flight 2, 2 August 1980, 19.09 LT.

turbations produced by the cell. Refraction and reflection have negligible effects on the actinic flux in the cell (Madronich *et al.* 1983). A correction, however, must be made to account for shadowing of parts of the cell volume by mechanical supports of the instrument and by insulating foam near the end flanges of the cell. This correction is (Madronich *et al.* 1983)

$$J_{NO_2} = \frac{J_M}{f_o w_o + f_u w_u + f_d w_d} \tag{3}$$

where f_i is the fraction of the total cell volume illuminated, and w_i is J_i/J_{NO_2}. The subscripts refer to the light component i ($i = o$ for direct, $i = u$ for up-scattered, and $i = d$ for downscattered actinic flux).

The weight factors, w_i, were estimated from an isotropic multiple scattering model for a spherical Earth geometry and are shown in Figure 5 for several altitudes as a function of the solar zenith angle. A global average surface albedo of 0.25, typical of partial cloud cover, was used for these calculations.

Values of f_i are specific to the geometry and orientation of the instrument. Since the direct solar beam casts a sharp shadow, f_o was determined from the geometry of the

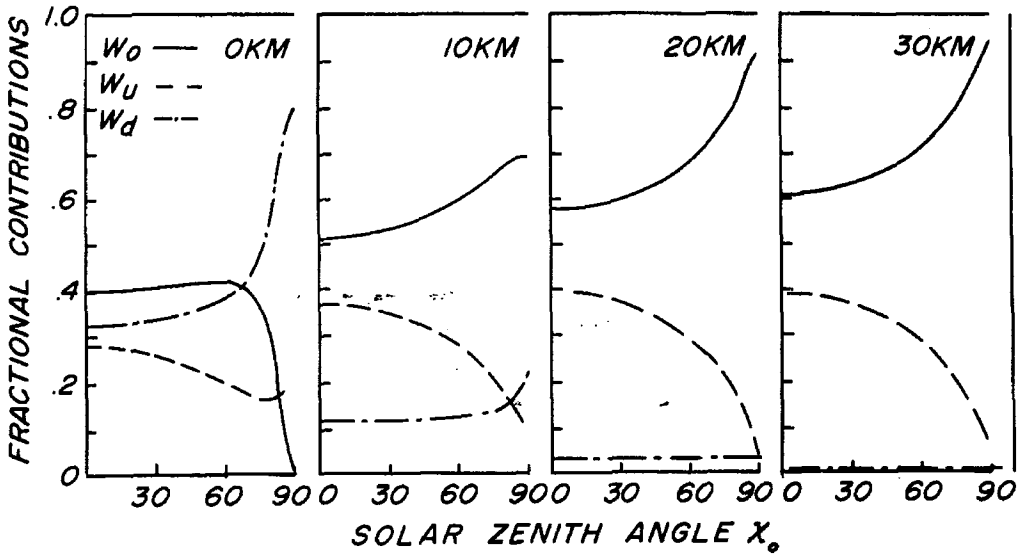

Fig. 5. Fractional contributors of J_{NO_2} calculated from the isotropic model for a surface albedo of 0.25. Direct Sun, w_o; downscattered radiation, w_d; upscattered radiation w_u.

fittings and the insulation surrounding the ends of the cell. For a vertical cell:

$$f_o = (0.88 \pm 0.01) - (0.037 \pm 0.006) \cot \chi_0 \quad \text{for } 30^\circ < \chi_0 < 90^\circ;$$
$$f_o = (0.95 \pm 0.01) - (0.079 \pm 0.010) \cot \chi_0 \quad \text{for } 5^\circ < \chi_0 < 30^\circ \qquad (4)$$

where χ_0 is the solar zenith angle.

The calculation of f_u and f_d is more complex because a knowledge of the angular distribution of the incoming fluxes is required. If both the upward and downward scattered light are assumed to vary only with azimuth, the average fraction of the cell volume that is illuminated by each component can be determined by integrating the unshadowed field of view along the axis of the cell (Madronich *et al.*, 1983). For the cell in the vertical position the calculations give:

$$f_u = 0.68 \pm 0.03 \qquad (5)$$
$$f_d = 0.87 \pm 0.02 \qquad (6)$$

A final adjustment to the measurements arises from the temperature dependence of J_{NO_2}. J_M is determined at an elevated cell temperature (Table I) compared to the ambient values of 226 and 237 K for flights 1 and 2, respectively. We have adjusted our measured J_{NO_2} values from the temperature of the warm cell to ambient temperature by a linear interpolation of the calculated temperature dependence of Madronich *et al.* (1984).

Uncertainties in the J_{NO_2} determination were estimated from (1) the precision and accuracy of the pressure measurements, ±2.2–11.0% (2) possible systematic errors due to the neglect of secondary kinetics (e.g., recombination, excited NO_2 reactions, N_2O_5 formation), ±2.5% (3) sensitivity tests on the cell cooling correction ±1.0–3.0% (flight 1 only); (4) the shadowing correction, ±1.6–2.6%; (5) maximum actinic flux attenua-

Table I. Stratospheric J_{NO_2} measurements

Local time (GMT-5 H)	Solar zenith angle (degrees)	Initial pressure (Torr)	Cell temperature (K)	J_M (10^3 s)	J_{NO_2} at cell temperature (10^3 s)	J_{NO_2} at ambient temperature (10^3 s)	J_{NO_2} uncertainty (%)
Flight 1: 22 July 1980, 24 km, Ambient Temperature = 226 K							
08:37	65.2	1.79	281	8.5	10.5	9.2	9
09:43	54.8	1.39	288	9.6	12.1	10.5	15
10:39	46.3	1.77	285	9.3	11.8	10.2	9
11.29	39.4	1.84	285	9.3	11.9	10.4	9
12.25	33.2	1.61	287	9.5	12.3	10.6	10
13:30	29.6	2.46	282	8.9	11.6	10.2	7
15:11	34.2	1.73	294	9.1	11.8	10.1	10
15:38	37.2	1.70	279	9.1	11.8	10.4	9
16:03	40.4	1.66	271	9.3	11.9	10.6	8
16:26	43.6	1.89	265	8.8	11.2	10.2	7
17:57	57.5	1.47	304	9.4	11.7	9.8	10
Flight 2: 2 Aug. 1980, 32 km, Ambient Temperature = 237 K							
15:55	43.2	1.23	274	9.0	11.4	10.5	10
16:29	47.8	1.39	272	9.2	11.7	10.8	9
17:25	55.8	1.54	285	9.2	11.6	10.3	10
18:08	62.1	1.41	283	9.6	11.8	10.6	10
18:42	67.8	1.16	278	8.4	10.3	9.3	11
19:07	71.7	2.10	275	9.0	10.9	10.0	7
19:35	76.1	2.77	271	8.9	10.6	9.8	6
20:08	81.2	1.46	267	7.8	9.3	8.6	7
20:46	86.1	1.38	266	7.2	8.3	7.8	7
21:13	90.3	1.22	263	6.4	7.0	6.1	7

tion due to the NO_2 in the cell <3%; and (6) the uncertainty in the J_{NO_2} temperature dependence adjustment <3%. The total uncertainty in J_{NO_2} ranged from ±6% to ±15%. The J_{NO_2} measurements and the conditions under which they were obtained are summarized in Table I.

6. Results and Discussion

The J_{NO_2} measurements obtained at 24 km altitude (flight 1) are shown in Figure 6a. Measurements obtained in the morning are, within the experimental uncertainty, indistinguishable from afternoon measurements obtained at similar zenith angles. For high Sun conditions ($28^\circ < \chi_0 < 50^\circ$), J_{NO_2} showed very little variation, with an average value of $(10.3 \pm 0.3) \times 10^{-3}$ s^{-1}. The measurement at the largest zenith angle attained during flight 1 ($\chi_0 = 65.2^\circ$) is about 10% smaller than the high Sun value.

The J_{NO_2} measurements obtained at 32 km altitude (flight 2) are shown in Figure 6b. For high Sun ($43.2^\circ < \chi_0 < 62.1^\circ$), J_{NO_2} values were constant to within the experimental uncertainty, with a mean value of $(10.5 \pm 0.3) \times 10^{-3}$ s^{-1}, or only about

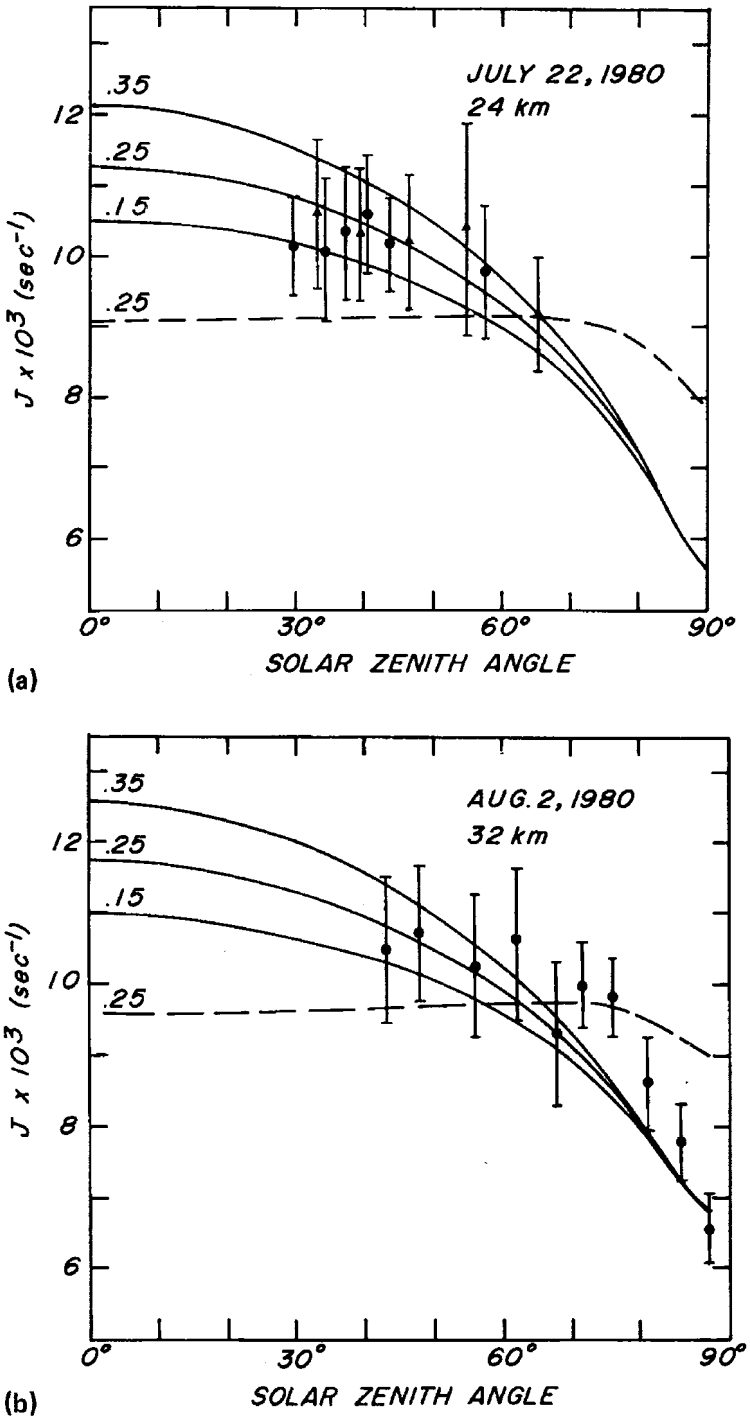

Fig. 6. Stratospheric J_{NO_2} values. Solid and dashed curves are isotropic and columnar model results respectively. Values of albedo are indicated. (a) Flight 1, 22 July 1980; (b) Flight 2, 2 August 1980.

2% higher than the values obtained for high Sun at 24 km altitude. The value of J_{NO_2} at 67.8° is about 10% lower than the high Sun values, a difference which is larger than the precision of the J_{NO_2} measurements. This J_{NO_2} decrease may be due to a change in

albedo, since this measurement was obtained in the time between the dissipation of cumulus clouds and the arrival of the cirrus formation (see Section 4). J_{NO_2} values obtained at solar zenith angles greater than about 75° show a monotonic decrease, down to a value of $(6.6 \pm 0.5) \times 10^{-3}$ s^{-1} at $\chi_0 = 90°$.

Several methods have been proposed to calculate J_{NO_2} from Equation (1). Two such methods, the 'columnar' scattering model of Isaksen *et al.* (1977) and the 'isotropic' scattering model of Luther (1980), were used to calculate J_{NO_2} values. Details of the calculations are given elsewhere (Madronich, 1982). Briefly, the two methods differ mainly by the inclusion, in the isotropic model, of the Lambertian factor of 2 cos χ_0 whenever direct sunlight is scattered by the Earth's surface or by an atmospheric layer, while the columnar calculation assumes specular scattering.

The results of the calculations for the two models are shown in Figure 6a and b together with the J_{NO_2} measurements. The isotropic calculation with an albedo of 0.25 is seen to give better overall agreement, to within 15% for all measurements. By contrast, the columnar calculation gives good agreement only for solar zenith angles near 60°, where the two theoretical methods are identical (since 2 cos $\chi_0 = 1$).

Most noticeably, the rapid decrease in measured J_{NO_2} values at zenith angles larger than 75° is not predicted by the columnar model, which therefore seriously overestimates J_{NO_2} at low Sun conditions. The isotropic model is in better agreement with the measurements for large zenith angles, but the measured decrease in J_{NO_2} as sunset is approached is marginally more pronounced than this model predicts. This discrepancy cannot be attributed to an improper choice of surface albedo in the calculations, since at large zenith angles the theoretical dependence of J_{NO_2} on albedo is very weak. For zenith angles in the range 30–60°, the values of J_{NO_2} calculated with the isotropic model are again in better agreement with the measurements, but the increase in J_{NO_2} with decreasing zenith angle, which is predicted by the isotropic theory, is not suggested by the measurements. The measurements of flight 1, in particular, suggest that J_{NO_2} may be only weakly dependent on zenith angle for $\chi_0 < 60°$, as predicted qualitatively by the columnar model.

Finally, the very weak dependence of measured J_{NO_2} values on altitude confirms the theoretical predictions. For example, the isotropic calculation shows that for $\chi_0 < 80°$, J_{NO_2} values obtained during flight 2 (32 km, 237 K) should be about 4% higher than J_{NO_2} values obtained from flight 1 (24 km, 226 K). This small altitude effect is attributed, in about equal proportions, to the altitude dependence of the actinic flux and to the temperature dependence of J_{NO_2}.

References

Isaksen, I. S. A., Midtbo, K. H., Sunde, J., and Crutzen, P. J., 1977, A simplified method to include molecular scattering and reflection in calculations of photon fluxes and photodissociation rates, *Geophys. Norveg.* **31**, 11–26.

JPL, 1982, Chemical kinetic and photochemical data for use in stratospheric modelling: Evaluation Number 5, JPL Publication 82–57, Pasadena, California.

Luther, F. M. and Gelinas, R. J., 1976, Effects of molecular multiple scattering and surface albedo on atmospheric photodissociation rates. *J. Geophys. Res.* **81**, 1125–1132.

Luther, F. M., 1980, Annual Report of the Lawerence Livermore National Laboratory to the FAA, UCRL-50042-80, Lawerence Livermore Laboratory, Livermore California.

Madronich, S., 1982, Measurements of the photodissociation coefficient of NO_2 in the stratosphere, PhD Thesis, York University.

Madronich, S., Hastie, D. R., Ridley, B. A., and Schiff, H. I., 1983, Measurement of the photodissociation coefficient of NO_2 in the atmosphere: I. Method and surface measurements, *J. Atmos. Chem.* **1**, 3–25.

Madronich, S., Hastie, D. R., Ridley, B. A., and Schiff, H. I., 1984, Calculations of the temperature dependence of the NO_2 photodissociation coefficient in the atmosphere, *J. Atmos. Chem.* **1**, 151–158.

Mugnai, A., Petroncelli, P., and Fiocco, G., 1979, Sensitivity of the photodissociation of NO_2, NO_3, HNO_3 and H_2O_2 on the solar radiation diffused by the ground and by atmospheric particles, *J. Atmos. Terr. Phys.* **41**, 351–359.

WMO, 1981, The stratosphere 1981: Theory and measurements, WMO Global Ozone Research and Monitoring Project, Report No. 11, May 1981.